Ferdinand Bammer* and Florian Huemer

Real-time imaging-ellipsometry on cylindrical substrates with a polarization camera

Abbildende Echtzeitellipsometrie auf zylindrischen Substraten mit einer Polarisationskamera

https://doi.org/10.1515/teme-2023-0119
Received August 21, 2023; accepted October 5, 2023;
published online November 15, 2023

Abstract: Based on a polarization camera we present an imaging-ellipsometer for inline quality control of thin layers within a thickness range of 0–500 nm. We describe the application to cylindrical substrates like bottles, tubes or foils on guide rolls in roll-to-roll-production. We demonstrate the new system for SiO_2-coated PET-bottles, PDMS-coated glass-tubes, and SiO_2-coated PET-foils. With frame rates of up to 24 fps the ellipsometer is aimed for both fast offline as well as real-time inline thickness-control.

Keywords: inline-imaging-ellipsometry; inline thickness measurement; R2R-printing

Zusammenfassung: Wir demonstrieren ein abbildendes Echtzeit-Ellipsometer, basierend auf einer Polarisationskamera. Das System kann für die Qualitätskontrolle von Beschichtungen im Dickenbereich 0–500 nm benutzt werden. Wir beschreiben die Anwendung an zylindrischen Proben, wie Flaschen, Rohre oder Folien auf Umlenkrollen in der Rolle-zu-Rolle-Produktion. Wir zeigen Messergebnisse des neuen Systems an SiO_2-beschichteten PET-Flaschen, PDMS-beschichteten Karpulen und SiO_2-beschichteten PET-Folien. Mit bis zu 24 Aufnahmen pro Sekunde werden sowohl schnelle Anwendungen im Labor als auch in Echtzeit in der Produktionslinie adressiert.

Schlagwörter: abbildende Echtzeit-Ellipsometrie; Echtzeit Dickenmessung; R2R-Druck

***Corresponding author: Ferdinand Bammer**, Technische Universität Wien, Institute of Production Engineering and Photonic Technologies, Getreidemarkt 9/311, 1060 Vienna, Austria,
E-mail: ferdinand.bammer@tuwien.ac.at. https://orcid.org/0000-0002-4037-4096
Florian Huemer, Technische Universität Wien, Institute of Production Engineering and Photonic Technologies, Getreidemarkt 9/311, 1060 Vienna, Austria, E-mail: fhuemer@ecs.tuwien.ac.at. https://orcid.org/0000-0002-2776-7768

1 Introduction

To address the increasing need in control of thickness of thin layers *in-situ* and in-time we examine and demonstrate the use of a polarization camera for ellipsometric inline measurements. It is long known that polarization cameras can be used for inline-imaging-ellipsometry. For example [1] proposed a fast imaging ellipsometer with a polarization camera based on a 3-camera-system with a linear polarization filter in front of each camera, with filter orientations 0, 60, and 120°. In [2] a different design is introduced based on one sensor with polarizers in front of each pixel, oriented at 0, 45, 90, and 135°. Current state of the art cameras are based on this design and use the Sony-CMOS-polarization sensor [3], with a nano wire grid in front of its sensor, segmented in 2×2-pixel-groups, where each group contains 4 polarizers of the above mentioned orientations. Several manufacturers offer polarization cameras based on this sensor. We work with the EXO250ZGE from the company VISTEK [4].

2 Measurement principle

In ellipsometry the sample (in most cases a substrate with one or more coatings, in this work we consider only one layer on a known substrate) is illuminated with 45° linear polarized collimated light with the angle of incidence (AOI) (Figure 1) close or equal to the Brewster-angle [5] of the substrate. The change of polarization imposed on the reflection by the sample is used to determine the properties of the coating, especially the layer thickness. This is because the reflection from a layer or layer system on a substrate is in fact the superposition of infinitely many partial reflections generated by all the extra surfaces in the coating system. Each single reflection has a different complex reflection coefficient. The superposition of all reflections, i.e. the interference of all reflected partial beams, results in a new polarization state of the reflected complete beam [5].

For illumination we use an LED, chosen with a wavelength λ that fits to the given task and is visible to the camera, i.e. λ is chosen in the range 350–1100 nm. The reflected light is imaged on a polarization camera. To address

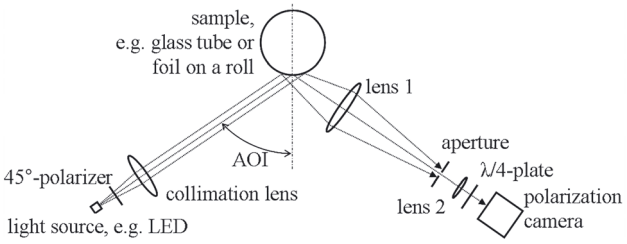

Figure 1: Optical setup.

thin layers with typically small refractive-index differences between layer and substrate we extend the measurement to circularly polarized light. This leads to a setup, which is very sensitive to the small phase-changes typically introduced by thin layers. Hence, we place a quarter-wave-plate in the light path after the reflection usually directly in front of the camera or alternatively in the common focal point of the two lenses of the imaging system (Figure 1). The fast axis of the quarter-wave-plate includes an angle of 45° with the drawing plane of Figure 1. This leaves the measurements of the 45°- and 135°-pixels unchanged (since 45°- and 135°-polarized light passes a 45°-positioned waveplate unchanged). The 0°- and 90°-polarized pixels are now measuring the left/right circular component of the beam (since 0°- and 90°-polarized light passing a 45°-positioned quarter-waveplate is transformed to left/right circularly polarized light). We call the measured intensities I_{45}, I_{135}, I_R, I_L and use them to define two ratios, which are in case of purely polarized light equal to the 3rd and 4th component of the normalized Stokes-vector [5]:

$$R_{45} = (I_{45} - I_{135})/(I_{45} + I_{135}) \tag{1}$$

$$R_Z = (I_R - I_L)/(I_R + I_L) \tag{2}$$

This ratiometric measurement is independent from the absolute intensity, which is of utmost importance for a robust optical measurement. Furthermore R_{45} and R_Z are highly dependent on layer-thickness. A similar approach was already proposed in [6], however in this setup the intensities were taken one after another, by fast polarization switching of the light source.

The dependence of R_{45} and R_Z on the layer thickness is strongly influenced by the chosen wavelength, which needs to be adapted to coating material and coating thickness. The thicker the coating the longer the wavelength needs to be.

The illumination is usually done with collimated light and hence the second important parameter is the illumination angle AOI. Usually, it is set equal or close to the Brewster-angle of the substrate, where the *p*-polarization (parallel polarization, i.e. linear polarized light with electric field parallel to the optical plane defined by the drawing plane in Figure 1) is not reflected, or at least has its reflection minimum. For the uncoated substrate R_{45} is equal to zero at the Brewster-angle since the corresponding intensities are equal. R_Z is for a non-absorbing uncoated substrate always zero, independent of the AOI. But it is very sensitive to even a small absorption of the substrate.

The calculation of the dependence of polarization of the reflected light on the properties of the layers is done with the matrix-transfer-method [5], which is implemented in the calculation programs of the providers of ellipsometers. We use the program 'EP4-model' of ACCURION [7], where parameters like refractive index and layer thickness are determined by a numbering matching procedure between mathematical model and measured data.

However for inline applications a simplified calculation is needed. For the simplest case, which is only considered in this work, the measurement of the thickness t of one layer on a substrate (all refractive indices known, absorption negligible), we use the approximations, with R_A … amplitude of R_Z-dependence and t_{ref} … reference thickness in nm:

$$R_Z = R_A \sin(\pi t/t_{ref}) \tag{3}$$

$$R_A - R_{45} = R_A \cos(\pi t/t_{ref}) \tag{4}$$

This is only a rough approximation as a comparison with real cases depicted in Figures 2 and 5 shows. However it proofed to be sufficient for inline applications, where first a lot of noise is present and second only rough estimations of the layer thickness and the evenness of its distribution are expected. From Equations (3) and (4) the thickness t can be directly calculated:

$$t = t_{ref}\,\mathrm{atan}(R_Z/(R_A - R_{45}))/\pi \tag{5}$$

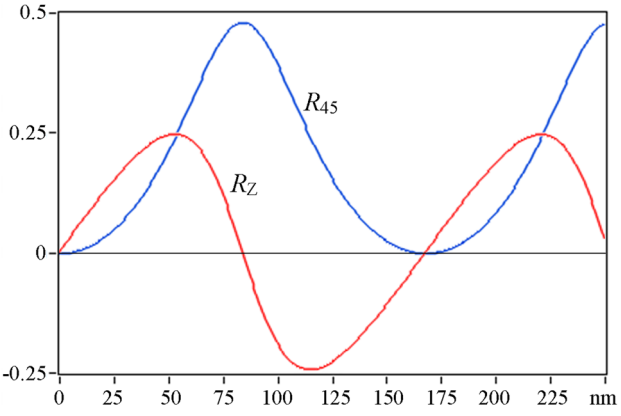

Figure 2: Dependence of R_{45} and R_z for SiO_2 on PET on the layer thickness with $\lambda = 400$ nm, AOI = 59.4°.

Theoretically this allows a unique measurement of t in the range 0–2 t_{ref}. Due to signal noise the true range is somewhat smaller.

3 Setup and results

Many important applications in quality control are on cylindrical surfaces. This is advantageous for imaging ellipsometry since the illumination of a cylindrical reflecting object with collimated light and imaging with an angle-sensitive (i.e. accepting only a small input angle variation) objective – typically a telecentric one – yields a sharply defined and stable line in the image, along which the thickness distribution can be measured in-line. Furthermore, transparent samples like PET-bottles or glass-tubes allow the measurement on the inner side, too.

Figure 1 shows the scheme of the optical setup. Collimated light with linear polarization of 45° (all orientations of polarizing optical elements are referred to the drawing plane of Figure 1, which is the optical plane, defined by the central incoming and central reflected light ray) is directed to a cylindrical sample and reflected as a diverging beam. The imaging system can in principle be quite general, but to ease the evaluation of the image it is advantageous, that it has only a small acceptance angle in the order of ∼1°. Figure 1 shows a simple and robust solution based on lens 1 and lens 2 mounted with a common optical focal point. To decrease the acceptance angle an aperture is placed in the common focal point. This is in fact a simple realization of a telecentric lens (objective).

In all the following examples imaging is done with two confocal lenses with focal lengths $f_1 = 200$ mm and $f_2 = 24$ mm. The resulting magnification is $f_2/f_1 = 0.12$. The quarter-wave-plate is positioned directly in front of the camera sensor (as shown in Figure 1) or in the common focal point of the two lenses, where also an additional small aperture can be placed to increase the angle-sensitivity of the imaging system.

3.1 SiO_2-layer on the inner side of PET-bottles

Avoiding loss of gas and flavors in PET-bottles needs special attention. One solution is to use plasma-coating to apply a SiO_2-layer with a thickness of ∼30 nm as a barrier on the inner side of the bottle. For this particular application quality control must be performed inline at a typical production speed of 14 bottles/s (∼50,000 bottles/h). The detection of the layer and of its thickness is difficult due to its transparency and due to the necessity to measure through the wall of the bottle. For this thickness-range a short wavelength was chosen at the edge of camera's sensitivity to be more sensitive for thin layers. We performed the experiments with an LED with center wavelength $\lambda = 400$ nm where the refractive indices are $n_{PET} = 1.693$ and $n_{SiO2} = 1.476$ [8]. This large refractive-index difference allows a stable ellipsometric measurement even through the wall of the bottle.

Figure 2 shows the strong dependence of R_{45} and R_z ($\lambda = 400$ nm, AOI = 59.4°, all calculations done with the Program EP4Model from the company ACCURION [7]) for SiO_2 on PET on the layer thickness.

The corresponding parameters for the thickness calculation with Equation (5) are $R_A = 0.23$ and $t_{ref} = 85$ nm. Obviously a measurement of both parameters allows a unique determination of the layer thickness in the range of 0–170 nm.

Figure 3 shows a laboratory setup for the measurement of the layer distribution in the bottle. A high power (max. current 350 mA) LED with center wavelength 400 nm is collimated with an aspheric lens and illuminates the bottle, which is mounted on a stepper motor. Due to the angle-selectivity of the objective it images only a small stripe (Figure 4) on the sensor, with a very clear polarized content from the inner layer, despite of the fact that it contains both the reflections from the outer uncoated and of the inner coated side.

Figure 4 shows 360°-scans on four coated bottles. The horizontal axis shows the number of measurements and the vertical axis shows the vertical height in mm. 650 sensor pixels correspond to 37 mm height of the label region, which is the only cylindrical part of the bottle, where imaging works properly.

On a single coated bottle 50 measurements were made during one 360° rotation. Additionally ∼20 measurements on three different uncoated bottles are displayed between. The acquisition time of the camera is 500 µs. One turnaround is finished in approx 5 s. The measured layer thickness is indicated by the color, with dark blue corresponding to 0 nm and yellow to ∼50 nm.

The results show a panoramic view of the thickness distribution inside the bottle and indicate clearly that the system can distinguish between uncoated and coated bottles and furthermore shows also the partially uneven thickness distribution. For example the 3rd coated bottle shows a very obvious thickness jump around the 20th measurement (measurement 160 in the horizontal scale). The validity of the measured distributions was confirmed with an imaging ellipsometer of type EP3 of the company ACCURION.

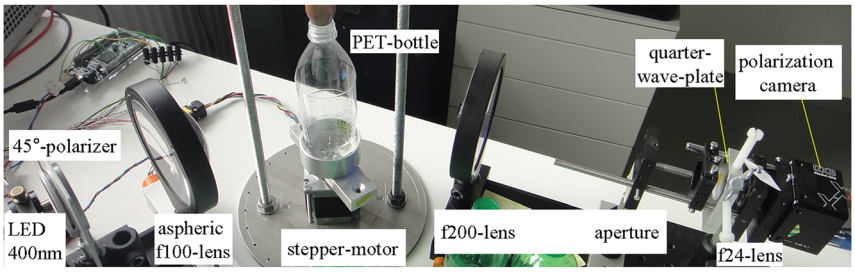

Figure 3: Setup for 360°-scans on PET-bottles.

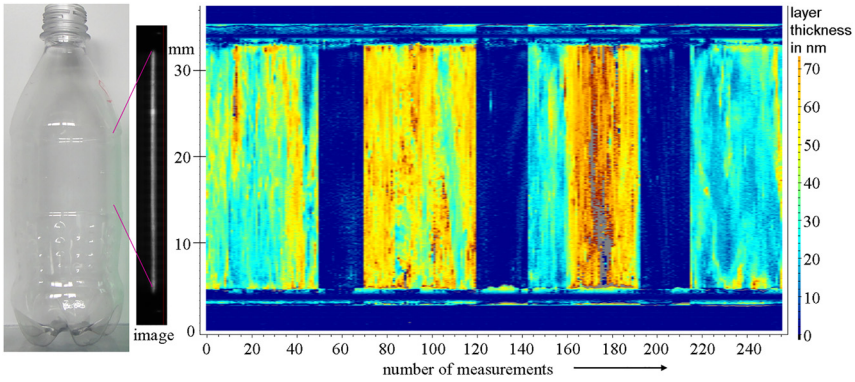

Figure 4: Thickness distribution in 4 different SiO_2-coated PET-bottles.

3.2 PDMS-layer on the inner side of glass-tubes

Here we deal with the coating of glass-tubes for syringes. The inner diameter of the tube is 9.6 mm, the outer diameter is 11.6 mm and hence the wall thickness is 1 mm.

To enable a smooth movement of a rubber-piston these tubes are coated on the inner side with a silicon-oil, of type PDMS (Polydimethylsiloxane). The thickness should be constant at ∼100 nm, but oscillates in reality between 0 and 350 nm. Due to this wide thickness range we use a long wavelength, i.e. $\lambda = 970$ nm, where strong LEDs are available and where the camera still has a sufficient spectral response.

Figure 5 shows the dependence of both ratios on the PDMS-thickness for $\lambda = 970$ nm and the corresponding AOI = 56.14°, which is the Brewster-angle of the glass, brand name Fiolax, with $n_{\text{glass, 970}} = 1.49$. The refractive index of PDMS is estimated to be (no valid data available) $n_{\text{PDMS, 970}} = 1.41$.

The corresponding parameters for the thickness calculation with Equation (5) are $R_A = 0.09$ and $t_{\text{ref}} = 210$ nm. The uniquely measurable thickness-range is here 0–420 nm. Note that, due to the quite small refractive index difference between layer and substrate the change of the two ratios is now nearly by a factor 3 smaller than in the previous example. However, here the reflections from the outer side and the inner side of the glass-tube are, due to the wall thickness, clearly separated and hence two thin lines are seen in the image (Figure 6). Due to this separation a reliable thickness-measurement is still possible.

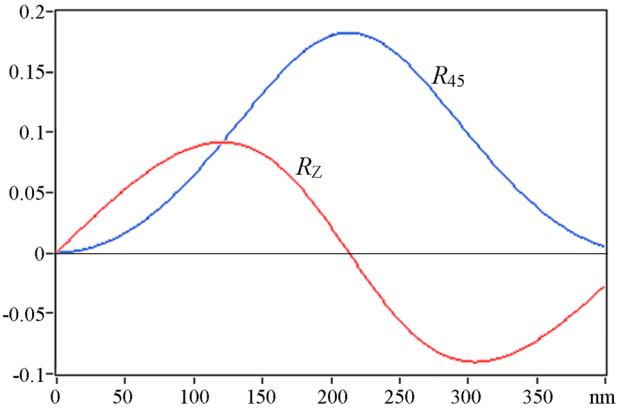

Figure 5: Dependence of R_{45} and R_z for PDMS on glass on the layer thickness with $\lambda = 970$ nm, AOI = 56.14°

Figure 6 again shows a panoramic view, produced with the setup of Figure 3 (modified to the longer wavelength 970 nm and with a different holder for the much smaller glass tubes)

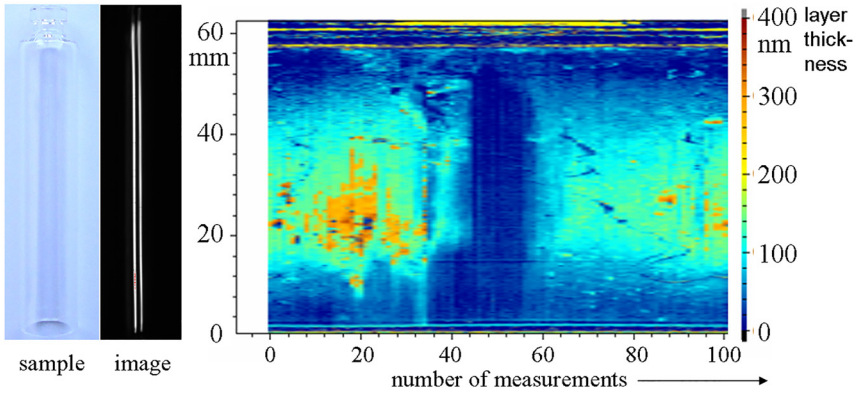

Figure 6: Thickness distribution on the inside of one PDMS-coated glass-tube.

The displayed result is from one coated glass-tube, fully rotated by 360°, with a measurement carried out every 3.6°, so altogether 100 measurements are displayed on the horizontal axis. The vertical axis shows the height in mm, and the color indicates the layer thickness. On the left hand side the sample and the corresponding image are displayed. The weaker line, here the right one, belongs to the reflection from the coated inner side.

The coating was removed partially with a cotton bud, which can be clearly seen as a dark blue area. The thickness distribution in this sample is very uneven and covers the range from 0–350 nm. Again one such measurement takes only some seconds, while conventional devices for PDMS-thickness-measurement, based on white light interferometry, can only measure one single spot in this duration.

3.3 SiO_2 on PET-foil

Again we consider SiO_2 on PET but this time with a foil as a substrate, which is used in production of e.g. flexible electronics based on printing roll-to-roll (R2R). These are difficult to access with inline-ellipsometry due to foil-vibrations and due to reflections from the backside of the foil, superposing an unknown polarization component (due to slightly varying thickness of the substrate and due to its tension-induced birefringence) indistinguishable from the main reflection. These problems can be reduced by measuring directly on a roll. Furthermore a short coherence length eliminates or at least significantly reduces the interference between the upside- and backside-reflection. Figure 7 shows the corresponding setup.

In this case the light source is a halogen lamp combined with a monochromator, set to the wavelength $\lambda = 633$ nm. The light is guided via a glass-fiber-bundle to the application. The light is then collimated with two cylindrical lenses (with focal length $f = 30$ mm and $f = 200$ mm) and illuminates the foil at AOI $= 58.6°$, the Brewster-angle of PET at $\lambda = 633$ nm. The foils are taped on a roll with 30 mm diameter.

As already seen in the example of coated PET-bottles, the influence of the reflection from the uncoated side can be sufficiently considered, if the ratios $R_{45\text{-ref}}, R_{Z\text{-ref}}$ for uncoated samples are used as a reference.

It is further important to note that a short coherence length as provided by an LED or a lamp is important. If the coherence length is longer than twice the substrate thickness, there would be interference between the 1st and 2nd reflection and hence even very small thickness-variations in the substrate thickness would disturb the measurement signal. For example 0.1 % thickness-variation for a 100 µm-substrate corresponds to a 100 nm-variation, which would cause very significant and erratic interference effects.

Figure 8 shows results for a 100 mm wide foil. The left hand side shows an uncoated foil. Both ratios are close to zero and are stored as references $R_{45\text{-ref}}$, $R_{Z\text{-ref}}$. The difference to this reference is then used to calculate the thickness

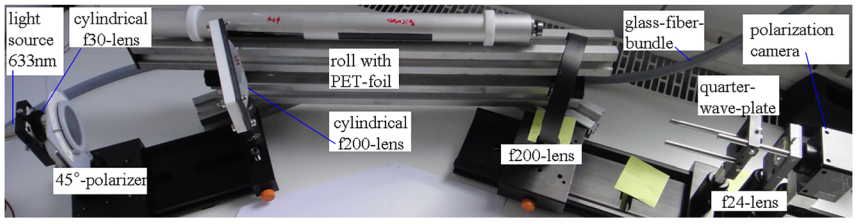

Figure 7: Setup for thickness measurement of a SiO_2-layer on a PET-foil.

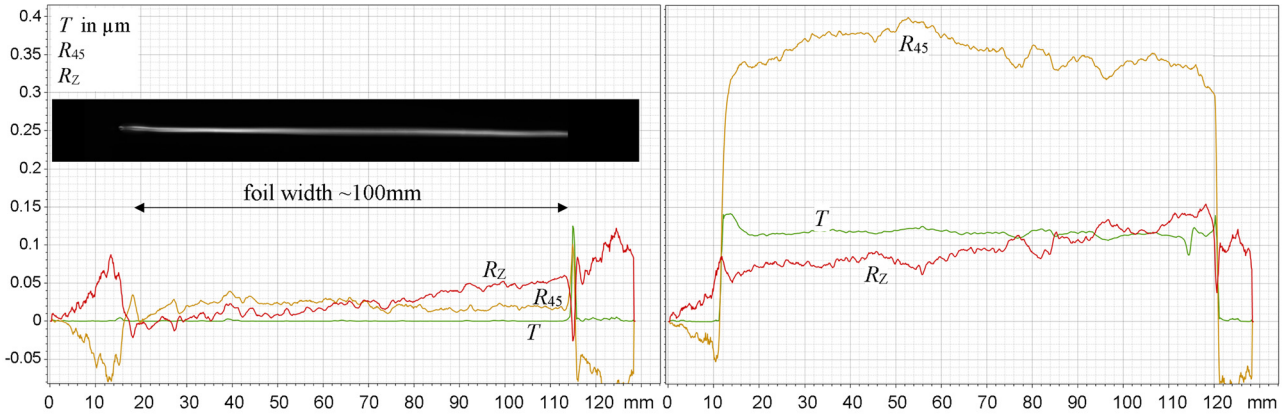

Figure 8: Measurement: SiO_2 on PET-Foil. Left: Uncoated (with real image inserted). Right: Coated.

T. This is seen on the right hand side, where a SiO_2-coated foil is analyzed. The change of the two ratios is very strong and the corresponding thickness is $T = \sim 120$ nm.

For the calculations the modified graphs of Figure 2 are used, due to the longer wavelength $\lambda = 633$ nm the unique measurement range is extended to a max. thickness of ~270 nm. Furthermore, the refractive indices are slightly smaller, i.e. $n_{\mathrm{PET},\,633} = 1.6388$ and $n_{\mathrm{SiO2},\,633} = 1.4626$ [8], and also the corresponding Brewster-angle of the uncoated substrate, which is now 58.6° and is hence also chosen here as the AOI.

The proposed setup can easily be installed on a R2R-line. The direct measurement on a roll allows for a very stable measurement and avoids problems with the waviness of the foil and with foil vibrations.

Due to the movement of the foil the thickness distribution of the complete coating can be acquired. E.g. with a camera speed of 24 fps and a typical foil velocity of ~25 mm/s there would be a longitudinal resolution of ~1 mm. The lateral resolution is 1200 px per width, so for a 100 mm wide foil the lateral resolution is ~0.1 mm.

4 Summary and outlook

We described a simple ellipsometric system based on a polarization camera that allows fast imaging ellipsometry and hence real-time measurements of the thickness distributions of thin layers in a thickness range of 0–500 nm, as demonstrated for SiO_2-coated PET-bottles, PDMS-coated glass-tubes, and SiO_2-coated PET-foils.

Future work will target installations in inline-applications. A straight-forward and cost-effective installation in production lines is to be expected, since the ellipsometer uses simple components and works without moving part on a fixed wavelength with a fixed illumination angle.

Acknowledgments: We would like to thank Dr. Berend Oberdorfer from the company SYNTEGON and Dr. Sebastian Kytzia from the company KHS. Further the scientific contributions from Dr. Dirk Hönig (company ACCURION) are gratefully acknowledged.
Research ethics: Not applicable.
Author contributions: The authors have accepted responsibility for the entire content of this manuscript and approved its submission.
Competing interests: The authors state no competing interests.
Research funding: None declared.
Data availability: The raw data can be obtained on request from the corresponding author.

References

[1] H. Korth, “Method and Apparatus for Determining the Polarization State of a Light Wave Field,” Patent US4516855A, 1982.
[2] S. Junger, W. Tschekalinskij, N. Verwaal, and N. Weber, “Polarization- and wavelength-sensitive sub-wavelength structures fabricated in the metal layers of deep submicron CMOS processes,” in *Proceedings of the SPIE conference on Nanophotonics III*, SPIE, 2010, p. 77120F–77129F.
[3] T. Yamazaki, Y. Maruyama, Y. Uesaka, et al., “Four-directional pixel-wise polarization CMOS image sensor using air-gap wire grid on 2.5-µm back-illuminated pixels,” *IEDM Conf. Proc.*, vol. 8, no. 7, supp. IEDM16, pp. 220–223, 2016.
[4] S. Weizmann, “Introduction to polarized cameras,” 2022. Available at: https://www.svs-vistek.com.
[5] H. G. Tompkins, *Handbook of Ellipsometry*, Heidelberg, Springer, 2004.
[6] F. Huemer, M. Jamalieh, F. Bammer, and D. Hönig, “Inline Imaging-Ellipsometer for printed electronics,” *J. Tech. Mess.*, vol. 83, no. 10, pp. 549–556, 2015.
[7] D. Hönig, “EP4Model manual,” 2009. Available at: https://accurion.parksystems.com.

[8] I. H. Malitson. “Interspecimen comparison of the refractive index of fused silica,” *J. Opt. Soc. Am.*, vol. 55, pp. 1205—1208, 1965. Available at: https://refractiveindex.info.

Bionotes

Ferdinand Bammer
Technische Universität Wien, Institute of Production Engineering and Photonic Technologies, Getreidemarkt 9/311, 1060 Vienna, Austria
ferdinand.bammer@tuwien.ac.at
https://orcid.org/0000-0002-4037-4096

Ferdinand Bammer, PhD, is a Senior Scientist at the Institute of Production Engineering and Photonic Technologies of TU Wien in Austria. His research is on fast imaging-ellipsometry for quality control in production lines. He designs and evaluates inline imaging ellipsometers for pharmacy, beverage industry, and steel industry.

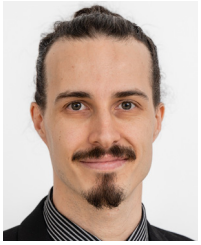

Florian Huemer
Technische Universität Wien, Institute for Computer Engineering, Treitlstraße 3, 1040 Vienna, Austria
fhuemer@ecs.tuwien.ac.at
https://orcid.org/0000-0002-2776-7768

Florian Huemer studied Computer Engineering at TU Wien in Austria, where he currently works as a Postdoc researcher in the Embedded Computing Systems group. His research interests include asynchronous and fault-tolerant circuit design with a special focus on quasi delay-insensitive circuits. Since 2013, he has been involved in several ellipsometry-based measurement engineering projects at the Institute of Production Engineering and Photonic Technologies at TU Wien.